

Drell-Yan process in soft-collinear effective theory near end-point

Jong-Phil Lee*

Department of Physics, Korea University, Seoul, 136-701, Korea

Abstract

The Drell-Yan process is analyzed in soft-collinear effective theory near the end-point region. It is assumed that the relevant final-state hadron energy $Q(1-z)$ where z is the momentum fraction transferred to the virtual photon is the typical hadronic scale $\sim \Lambda$, thus no intermediate scale exists. It is shown that this setup successfully reproduces the full theory results. We also discuss the factorized soft Wilson lines for the Drell-Yan process.

PACS numbers: 12.38.Bx,13.85.Hd

arXiv:hep-ph/0512348v2 2 Mar 2006

*Electronic address: jongphil@korea.ac.kr

I. INTRODUCTION

Hard scattering processes such as Drell-Yan (DY), and deep inelastic scattering (DIS) are receiving increased attention again nowadays with the development of effective theories.

There are two important issues for the processes. One is factorization. In short, factorization is a separation of long and short distance physics. Usually transition amplitudes for some processes are given by a factorized product or a convolution of hard and soft contributions when the factorization holds. The hard part is involved with the short distance physics which can be perturbatively calculated. Long distance physics is encoded with the soft contribution. In many cases, it is parametrized by the matrix elements of some operators. Factorization is in general very nontrivial in the full theory [1]. But the advent of the soft-collinear effective theory (SCET) [2] makes it very simple and automatic.

The other is the threshold resummation in the end-point region. By end-point, we mean $z \rightarrow 1$ where z is the usual momentum fraction. It has been quite well known that there are Sudakov double logarithms $[\alpha_s \ln^2(1-z)]^n$. In the end-point region, the large logarithm compensates the small strong coupling constant [3]. The origin of this singularity is the interaction between energetic partons and soft gluons. The resummation of these logarithms is necessary and also well studied [4]. Factorization is again a useful tool in this step [5]. One merit of factorization is that the factorized soft part is universal for soft emissions. In [6, 7], soft contributions are given by the vacuum expectation value of Wilson loops. The renormalization group evolution of the soft part is governed by the cusp anomalous dimensions which originate from the cusp angles in the Wilson lines. In position space, the cusp angles are well defined geometrically. They are responsible for the cusp divergences that give one logarithm of \ln^2 . The other log comes from the light-cone divergences of cusp angles which are proportional to $\sim \ln x^2$ where x is a light-like segment [8].

There have been several works for application of SCET to DIS and DY processes [9, 10, 11, 12, 13]. An interesting kinematic point is $\mu^2 \sim Q^2(1-z) \sim Q\Lambda$ where Λ is the hadronic scale. This so-called "hard-collinear" scale [14, 15] appears when soft and collinear particles interact. The hierarchy $Q^2 \gg Q\Lambda \gg \Lambda^2$ ensures the scale separation into hard, hard-collinear, and soft parts. By two-step matching [16], one can establish the low energy effective theory at $\mu \sim \Lambda$. Here since the intermediate scale $Q\Lambda$ is still large, it is integrated out to form the jet functions.

In SCET the factorization is automatic at the operator level. Especially, the soft gluon effects are compactly factorized in the soft Wilson line Y . In many hard scattering processes a universal feature of the soft gluon effects appears in the proper combination of Y s. Their properties are thoroughly studied in [11].

There is a slight difference between DIS and DY. In DIS the final state hadron carries the energy $\sim Q\sqrt{1-z}$ while that in DY is $\sim Q(1-z)$. In terms of the moments, the Sudakov double logs are minimized at $\mu = Q/\sqrt{N}$ for DIS and $Q = Q/N$ for DY where N is the order of moment.

In DIS, it is quite natural to define a jet function whose momentum scales as $\sim \sqrt{Q\Lambda}$. The forward scattering amplitude of DIS is connected with the quark lines and the intermediate line can be shrunk at the second step of matching by integrating out the large off-shellness $p_X^2 \sim Q^2(1-z) \sim Q\Lambda$, which defines unambiguously the jet function [2, 11]:

$$\langle 0|T [W^\dagger\psi(x) \bar{\psi}W(0)] |0\rangle \equiv i \int \frac{d^4k}{(2\pi)^4} e^{-ik\cdot x} J_P(k) \frac{\not{k}}{2}, \quad (1)$$

where W is the collinear Wilson line and J_P is the jet function. On the other hand, in DY there is no final-state hadron at $\mathcal{O}(\alpha_s^0)$, nor the hard-collinear scale which defines the intermediate theory SCET_I [11].

In this paper, we do not consider the intermediate scale to separate SCET_I and SCET_{II} for DY. Instead, the full QCD is directly matched onto the final effective theory at $\mu = Q$. The end-point region is defined by $1-z \sim \Lambda/Q \ll 1$, so the energy of final-state hadron $Q(1-z)$ is a small quantity. This is slightly different from the recent analysis on DY in SCET of [12], where $\mu \sim Q(1-z)$ is a large intermediate scale and two step matching is implemented. The main calculation of [12], which is for the soft gluon exchange diagram, is very similar to the full QCD analysis of [3]. In this work, the same diagram is calculated in a more SCET-based way. An alternative for the soft gluon effects is the use of soft Wilson lines developed in [11, 17]. At $\mathcal{O}(\alpha_s)$ all the soft gluon effects are contained in the factorized single gluon loop. It is shown how the new approach gives the same result.

The paper is organized as follows. Next Section deals with the basic kinematics and viewpoints on the application of SCET to DY. In Section III, the QCD electromagnetic current is matched onto the SCET current at $\mu = Q$, and the renormalization of four-quark operator is given. The factorized soft Wilson line approach appears in Sec. IV. The results of Sec. III is reproduced from the time ordered product of soft Wilson lines. In Sec. V,

the renormalization group evolution and resummation of double logarithms are given. The cancellation of μ -dependence in the cross section is discussed, and conclusions are added.

II. PRELIMINARY

A. Kinematics

The center-of-momentum frame of incident hadrons is a natural choice to describe DY. For the production of highly virtual photon whose invariant mass is $Q^2 > 0$, a parameter z defined by the ratio of Q^2 to the invariant mass of partons governs the kinematics. Explicitly,

$$(p_1 + p_2)^2 = 2p_1 \cdot p_2 \equiv s \equiv \frac{Q^2}{z}, \quad (2)$$

where $p_{1,2}$ are the incident partons' momenta. We assume they are massless. The end-point (or threshold) region is where $z \rightarrow 1$. It is quite convenient to introduce two light-like vectors n^μ and \bar{n}^μ where

$$n^\mu = (1, 0, 0, 1), \quad \bar{n}^\mu = (1, 0, 0, -1). \quad (3)$$

They satisfy $n^2 = \bar{n}^2 = 0$, $n \cdot \bar{n} = 2$. A momentum p can be decomposed as

$$p^\mu = n \cdot p \frac{\bar{n}^\mu}{2} + \bar{n} \cdot p \frac{n^\mu}{2} + p_\perp = (n \cdot p, p_\perp, \bar{n} \cdot p) = (p^+, p_\perp, p^-). \quad (4)$$

We choose $p_1(p_2)$ is $\bar{n}(n)$ -collinear:

$$\begin{aligned} p_1^\mu &= n \cdot p_1 \frac{\bar{n}^\mu}{2} = (n \cdot p_1, 0, 0), \\ p_2^\mu &= \bar{n} \cdot p_2 \frac{n^\mu}{2} = (0, 0, \bar{n} \cdot p_2). \end{aligned} \quad (5)$$

Since $s \approx Q^2$ in the end-point region, the photon momentum q can be set as

$$q^\mu = (Q, 0, Q), \quad (6)$$

where $Q = \sqrt{q^2}$. Define

$$x_1 \equiv \frac{Q^2}{2p_1 \cdot q}, \quad x_2 \equiv \frac{Q^2}{2p_2 \cdot q}, \quad (7)$$

then we have

$$\begin{aligned} n \cdot p_1 &= \frac{Q}{x_1}; & p_1 &= \left(\frac{Q}{x_1}, 0, 0 \right) \\ \bar{n} \cdot p_2 &= \frac{Q}{x_2}; & p_2 &= \left(0, 0, \frac{Q}{x_2} \right). \end{aligned} \quad (8)$$

Thus the final state hadron momentum p_X is

$$p_X = p_1 + p_2 - q = Q \left(\frac{1-x_1}{x_1}, 0, \frac{1-x_2}{x_2} \right), \quad (9)$$

and its invariant mass is

$$p_X^2 = Q^2 \frac{(1-x_1)(1-x_2)}{x_1 x_2} = Q^2 \left(\frac{1}{z} + 1 - \frac{1}{x_1} - \frac{1}{x_2} \right), \quad (10)$$

where the relation $z = x_1 x_2$ is used.

The momenta of mother hadrons are

$$\begin{aligned} P_1 &= \frac{p_1}{\xi_1} = (\sqrt{S}, 0, 0), \\ P_2 &= \frac{p_2}{\xi_2} = (0, 0, \sqrt{S}), \end{aligned} \quad (11)$$

where $\xi_{1,2}$ are momentum fractions and S is the hadronic invariant mass square. s and S are related by

$$s = (p_1 + p_2)^2 = (\xi_1 P_1 + \xi_2 P_2)^2 = \xi_1 \xi_2 S, \quad (12)$$

and

$$z = \frac{Q^2}{s} = \frac{Q^2}{\xi_1 \xi_2 S} \equiv \frac{\tau}{\xi_1 \xi_2}, \quad (13)$$

where $\tau \equiv Q^2/S$.

B. SCET

SCET is an effective theory for energetic and light particles. With the kinematics given above, the incident partons are successfully described by effective fields of SCET. We choose $\chi_{\bar{n}}$ for \bar{n} -collinear antiquark whose momentum is p_1 , and ξ_n for n -collinear quark with momentum p_2 . Here $\chi_{\bar{n}}$ and ξ_n are the standard collinear quark fields of SCET.

The relevant energy scales of DY at the end-point are Q and $Q(1-z)$. We assume that $1-z \sim \Lambda/Q$ where Λ is a typical hadronic scale. In this case the final state hadron has $p_X^2 = Q^2(1-z)^2 \sim \Lambda^2$. It must be compared with the DIS near end-point where the scattered-off parton by an energetic photon carries $p_{X_{\text{DIS}}}^2 = Q^2(1-x) \sim Q\Lambda$. The scale $\sqrt{Q\Lambda}$ is still larger than Λ , and one introduces an intermediate theory (SCET_I) to integrate out $\sqrt{Q\Lambda}$. The resulting final theory, SCET_{II}, is designed to describe only modes with virtuality of order Λ^2 .

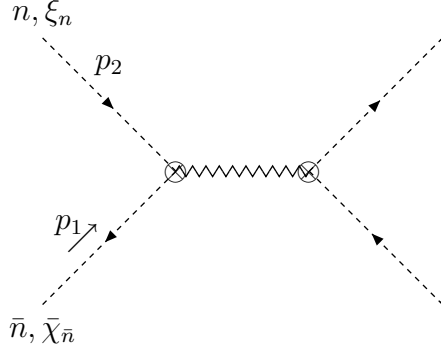


FIG. 1: Tree diagram of DY process in SCET.

On the other hand, since $Q(1-z) \sim \Lambda$ in DY, there is no intermediate scale to be integrated out, and thus no intermediate theory is needed. A direct matching from QCD to SCET at $\mu = Q$ will be enough for DY process at the end-point. This approach is quite different from that of [12], where they considered $Q(1-z)$ as still a large scale compared to Λ .

III. MATCHING AND RENORMALIZATION

At the scale $\mu = Q$, the electromagnetic current in full QCD $\bar{q}_1 \gamma^\mu q_2$ is matched onto the SCET current $\bar{\chi}_{\bar{n}} \gamma^\mu \xi_n$. At tree level, the matching is simple, and the matching coefficient $C(\mu)$ is just unity. Thus the tree level diagram of forward scattering amplitude (Fig. 1) gives

$$i\mathcal{A}^{\text{tree}} = (\bar{\xi}_n \gamma^\mu \chi_{\bar{n}}) \frac{-ig_{\mu\nu}}{(p_1 + p_2)^2 - Q^2 + i0^+} (\bar{\chi}_{\bar{n}} \gamma^\nu \xi_n). \quad (14)$$

Here the photon is considered as "massive" one whose invariant mass square is Q^2 , and $i0^+$ indicates the complex pole position. Since $(p_1 + p_2)^2 = 2p_1 \cdot p_2 = s = Q^2/z$, the discontinuity of $\mathcal{A}^{\text{tree}}$ is

$$\frac{1}{2\pi i} \text{Disc.} \mathcal{A}^{\text{tree}} = (\bar{\xi}_n \gamma^\mu \chi_{\bar{n}}) (\bar{\chi}_{\bar{n}} \gamma_\mu \xi_n) \frac{1}{Q^2} \delta(1-z). \quad (15)$$

The corresponding differential cross section is

$$\begin{aligned} 2s \frac{d\sigma}{dQ^2} &= \frac{1}{i} \text{Disc.} \mathcal{A}^{\text{tree}} \\ &= \frac{2\pi}{Q^2} \delta(1-z) (\bar{\xi}_n \gamma^\mu \chi_{\bar{n}}) (\bar{\chi}_{\bar{n}} \gamma_\mu \xi_n). \end{aligned} \quad (16)$$

This is the same as the full QCD result [3] up to the overall normalization.

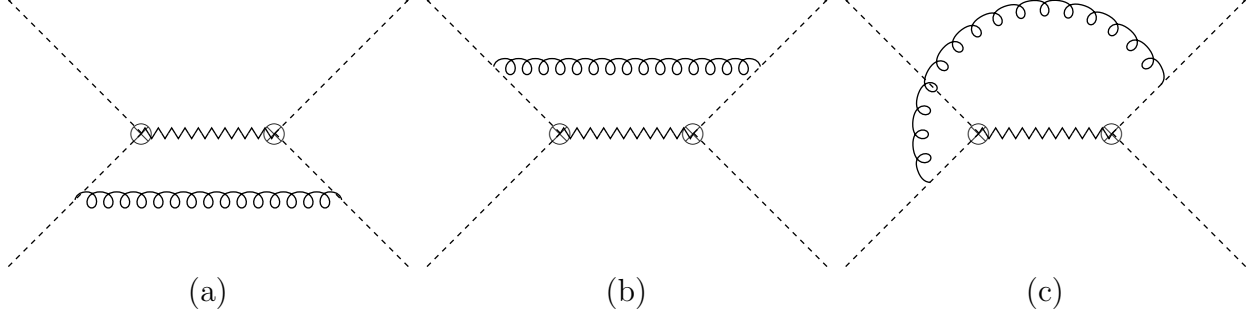


FIG. 2: Soft-gluon one-loop diagrams for DY process in SCET. Diagram (c) has its mirror image.

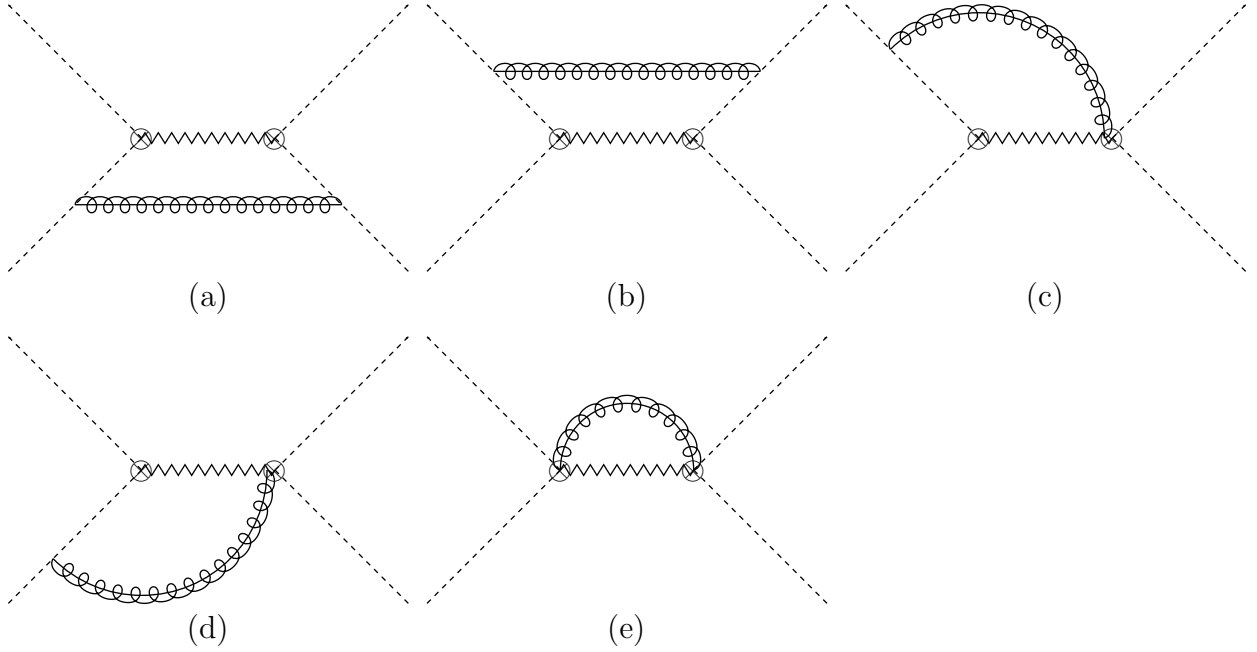


FIG. 3: Collinear-gluon one-loop diagrams for DY process in SCET. Diagrams (c) and (d) have their mirror images, and (e) contains n - and \bar{n} -collinear gluons.

At one-loop level, $C(\mu)$ is also already known in the literature [10]:

$$C(\mu) = 1 + \frac{\alpha_s}{4\pi} C_F \left(-\ln^2 \frac{\mu^2}{Q^2} - 3 \ln \frac{\mu^2}{Q^2} - 8 + \frac{7\pi^2}{6} \right). \quad (17)$$

Note that the current matching condition is given by the vertex corrections. The remaining one-loop diagrams for the forward scattering amplitudes are shown in Fig. 2 and Fig. 3. All these diagrams are responsible for the renormalization of effective four-quark operator.

Diagrams Fig. 2 (a) and (b) are proportional to $\sim \bar{n}^2$ or $\sim n^2$, thus vanish. Nontrivial contribution of the soft gluon comes from Fig. 2 (c). This diagram is already calculated in [12]. But the calculation is basically not different from the full QCD analysis of [3]. Here we

show how the SCET calculation of Fig. 2 (c) is implemented in detail and gives the same result as [3, 12]. Explicitly,

$$\begin{aligned}
i\mathcal{A}_{\text{sg(c)}} &= \int \frac{d^d\ell}{(2\pi)^d} \bar{\xi}_n \left(igT^a n^\alpha \frac{\not{\ell}}{2} \right) \frac{i\not{\ell}}{2} \frac{\bar{n} \cdot (p_2 + \ell)}{(p_2 + \ell)^2 + i0^+} \gamma^\mu \chi_{\bar{n}} \\
&\quad \times \bar{\chi}_{\bar{n}} \left(igT^b \bar{n}^\beta \frac{\not{\ell}}{2} \right) \frac{i\not{\ell}}{2} \frac{n \cdot (-p_1 - \ell)}{(p_1 + \ell)^2 + i0^+} \gamma^\nu \xi_n \\
&\quad \times \frac{-ig_{\mu\nu}}{(p_1 + p_2 + \ell)^2 - Q^2 + i0^+} \frac{-ig_{\alpha\beta} \delta^{ab}}{\ell^2 + i0^+} \\
&= 2g^2 C_F (\bar{\xi}_n \gamma^\mu \chi_{\bar{n}}) (\bar{\chi}_{\bar{n}} \gamma_\mu \xi_n) \cdot I_{\text{sg(c)}} , \tag{18}
\end{aligned}$$

where

$$\begin{aligned}
I_{\text{sg(c)}} &\equiv \int \frac{d^d\ell}{(2\pi)^d} \frac{1}{\ell^2 + i0^+} \frac{1}{(p_1 + p_2 + \ell)^2 - Q^2 + i0^+} \frac{n \cdot (p_1 + \ell)}{(p_1 + \ell)^2 + i0^+} \frac{\bar{n} \cdot (p_2 + \ell)}{(p_2 + \ell)^2 + i0^+} \\
&= \frac{1}{2} \int \frac{d\ell^+}{2\pi} \frac{d\ell^-}{2\pi} \frac{d^{d-2}\vec{\ell}_\perp}{(2\pi)^{d-2}} \frac{1}{\ell^+ \ell^- - \vec{\ell}_\perp^2 + i0^+} \frac{1}{(\ell^+ + p_1^+) (\ell^- + p_2^-) - \vec{\ell}_\perp^2 - Q^2 + i0^+} \\
&\quad \times \frac{\ell^+ + p_1^+}{(\ell^+ + p_1^+) \ell^- - \vec{\ell}_\perp^2 + i0^+} \frac{\ell^- + p_2^-}{\ell^+ (\ell^- + p_2^-) - \vec{\ell}_\perp^2 + i0^+} . \tag{19}
\end{aligned}$$

Since the gluon momentum ℓ is soft,

$$p_1^+, p_2^- \gg \ell^\pm, \sqrt{\vec{\ell}_\perp^2} , \tag{20}$$

and the integral becomes

$$\begin{aligned}
I_{\text{sg(c)}} &= \frac{1}{2} \int \frac{d\ell^+}{2\pi} \frac{d\ell^-}{2\pi} \frac{d^{d-2}\vec{\ell}_\perp}{(2\pi)^{d-2}} \frac{1}{\ell^+ \ell^- - \vec{\ell}_\perp^2 + i0^+} \frac{1}{(\ell^+ + p_1^+) (\ell^- + p_2^-) - \vec{\ell}_\perp^2 - Q^2 + i0^+} \\
&\quad \times \frac{p_1^+}{p_1^+ \ell^- + i0^+} \frac{p_2^-}{\ell^+ p_2^- + i0^+} . \tag{21}
\end{aligned}$$

In the photon propagator we keep all the components of ℓ^μ since $p_1^+ p_2^- \approx Q^2$. It is convenient to do first the contour integral over ℓ^+ . All the poles except that in the first term lie in the lower-half plane of complex ℓ^+ plane when $\ell^- < 0$ and $\ell^- + p_2 > 0$. Choosing the contour to cover the upper-half plane,

$$I_{\text{sg(c)}} = \frac{i}{2} \int_\theta \frac{d\ell^-}{2\pi} \frac{d^{d-2}\vec{\ell}_\perp}{(2\pi)^{d-2}} \frac{1}{p_2^- \vec{\ell}_\perp^2 + p_1^+ \ell^- (\ell^- + p_2^-) - Q^2 \ell^- - i0^+} \frac{1}{\vec{\ell}_\perp^2} , \tag{22}$$

where

$$\int_\theta d\ell^- \equiv \int d\ell^- \theta(-p_2^- < \ell^- < 0) . \tag{23}$$

Before proceeding, note that the discontinuity of $\mathcal{A}_{\text{sg}(c)}$ is

$$\frac{1}{i} \text{Disc.} \mathcal{A}_{\text{sg}(c)} = -2g^2 C_F (\bar{\xi}_n \gamma^\mu \chi_{\bar{n}}) (\bar{\chi}_{\bar{n}} \gamma_\mu \xi_n) \frac{1}{i} \text{Disc.} [iI_{\text{sg}(c)}] . \quad (24)$$

It is quite convenient to take the discontinuity in advance before doing the integration:

$$\begin{aligned} & \frac{1}{i} \text{Disc.} [iI_{\text{sg}(c)}] \\ &= -\frac{1}{2} \int_\theta d\ell^- \frac{d^{d-2} \vec{\ell}_\perp}{2\pi (2\pi)^{d-2}} \left(\frac{2\pi i}{i} \right) \delta \left[p_2^- \vec{\ell}_\perp^2 + p_1^+ \ell^- (\ell^- + p_2^-) - Q^2 \ell^- \right] \frac{1}{\vec{\ell}_\perp^2} \\ &= -\frac{1}{2} \int_\theta d\ell^- \left[\frac{1}{(4\pi)^{d/2-1}} \frac{1}{\Gamma(d/2-1)} d\vec{\ell}_\perp^2 \left(\vec{\ell}_\perp^2 \right)^{\frac{d-4}{2}} \right] \frac{1}{p_2^-} \delta \left[\vec{\ell}_\perp^2 - \frac{Q^2 - p_1^+ (\ell^- + p_2^-)}{p_2^-} \ell^- \right] \frac{1}{\vec{\ell}_\perp^2} \\ &= -\frac{1}{2p_2^-} \int_\theta d\ell^- \frac{1}{(4\pi)^{1-\epsilon}} \frac{1}{\Gamma(1-\epsilon)} \left[\frac{Q^2 - p_1^+ (\ell^- + p_2^-)}{p_2^-} \ell^- \right]^{-1-\epsilon} \theta \left(\frac{Q^2 - p_1^+ p_2^-}{p_1^+} < \ell^- < 0 \right) \\ &= -\frac{1}{2} \frac{1}{(4\pi)^{d/2-1}} \frac{1}{\Gamma(d/2-1)} (p_1^+ p_2^-)^{-1-\epsilon} \left(1 - \frac{Q^2}{p_1^+ p_2^-} \right)^{-1-2\epsilon} \int_0^1 dx (1-x)^{-1-\epsilon} x^{-1-\epsilon} . \quad (25) \end{aligned}$$

Since $p_1^+ p_2^- = (p_1 + p_2)^2 = s = Q^2/z$, the whole discontinuity is

$$\begin{aligned} & \frac{1}{i} \text{Disc.} (\mathcal{A}_{\text{sg}(c)} + \text{mirror}) \\ &= \left(\frac{2\pi}{s} \right) O_{DY} \left(\frac{g^2 C_F}{8\pi^2} \right) \left(\frac{4\pi\mu^2}{Q^2} \right)^\epsilon 2z^\epsilon (1-z)^{-1-2\epsilon} \frac{\Gamma^2(-\epsilon)}{\Gamma(1-\epsilon)\Gamma(-2\epsilon)} , \quad (26) \end{aligned}$$

where $O_{DY} = (\bar{\xi}_n \gamma^\mu \chi_{\bar{n}}) (\bar{\chi}_{\bar{n}} \gamma_\mu \xi_n)$. The calculation might have been much easier if the so called cutting rules were applied from the beginning :

$$\begin{aligned} & \frac{1}{i} \text{Disc.} [iI_{\text{sg}(c)}] \\ &= \frac{1}{2} \int \frac{d\ell^+ d\ell^-}{2\pi} \frac{d^{d-2} \vec{\ell}_\perp}{2\pi (2\pi)^{d-2}} (-2\pi i) \delta(\ell^+ \ell^- - \vec{\ell}_\perp^2) (-2\pi i) \delta \left[(\ell^+ + p_1^+) (\ell^- + p_2^-) - \vec{\ell}_\perp^2 - Q^2 \right] \\ & \quad \times \frac{\ell^+ + p_1^+}{(\ell^+ + p_1^+) \ell^- - \vec{\ell}_\perp^2} \frac{\ell^- + p_2^-}{\ell^+ (\ell^- + p_2^-) - \vec{\ell}_\perp^2} . \quad (27) \end{aligned}$$

It is very easy to see that Eq. (27) yields the same result as Eq. (25).

Similar manipulations can be done for the collinear gluon exchanges. Collinear contribu-

tion of Fig. 3 (a) is

$$\begin{aligned}
i\mathcal{A}_{\text{cg(a)}} &= \int \frac{d^d\ell}{(2\pi)^d} \bar{\xi}_n \gamma^\mu \frac{i\not{\ell}}{2} \frac{n \cdot (p_1 + \ell)}{(p_1 + \ell)^2 + i0^+} igT^a \\
&\times \left[\bar{n}_\alpha + \frac{\gamma_\alpha^\perp (\not{p}_1^\perp + \not{\ell}_\perp)}{n \cdot (p_1 + \ell)} + \frac{\not{p}_1^\perp \gamma_\alpha^\perp}{n \cdot p_1} - \frac{\not{p}_1^\perp (\not{p}_1^\perp + \not{\ell}_\perp)}{n \cdot (p_1 + \ell)} \frac{n_\alpha}{n \cdot p_1} \right] \frac{\not{\ell}}{2} \chi_{\bar{n}} \\
&\times \bar{\chi}_{\bar{n}} igT^b \left[\bar{n}_\beta + \frac{\gamma_\beta^\perp \not{p}_1^\perp}{n \cdot p_1} + \frac{(\not{p}_1^\perp + \not{\ell}_\perp) \gamma_\beta^\perp}{n \cdot (p_1 + \ell)} - \frac{(\not{p}_1^\perp + \not{\ell}_\perp) \not{p}_1^\perp}{n \cdot p_1 n \cdot (p_1 + \ell)} n_\beta \right] \frac{\not{\ell}}{2} \\
&\times \frac{i\not{\ell}}{2} \frac{n \cdot (p_1 + \ell)}{(p_1 + \ell)^2 + i0^+} \gamma^\nu \xi_n \\
&\times \frac{-ig_{\mu\nu}}{(p_1 + p_2 + \ell)^2 - Q^2 + i0^+} \frac{-ig^{\alpha\beta} \delta^{ab}}{\ell^2 + i0^+} \\
&= -g^2 C_F (\bar{\xi}_n \gamma^\mu \gamma_\perp^\alpha \gamma^\rho \chi_{\bar{n}}) (\bar{\chi}_{\bar{n}} \gamma_\rho \gamma_\alpha^\perp \gamma_\mu \xi_n) I_{\text{cg(a)}} , \tag{28}
\end{aligned}$$

where

$$I_{\text{cg(a)}} = \int \frac{d^d\ell}{(2\pi)^d} \frac{-\vec{\ell}_\perp^2}{d-2} \frac{1}{\ell^2 + i0^+} \frac{1}{(p_1 + p_2 + \ell)^2 - Q^2 + i0^+} \left[\frac{1}{(p_1 + \ell)^2 + i0^+} \right]^2 . \tag{29}$$

The discontinuity of $I_{\text{cg(a)}}$ is

$$\begin{aligned}
&\frac{1}{i} \text{Disc.} [iI_{\text{cg(a)}}] \\
&= \frac{1}{2} \int \frac{d\ell^+}{2\pi} \frac{d\ell^-}{2\pi} \frac{d^{d-2}\vec{\ell}_\perp}{(2\pi)^{d-2}} (-2\pi i) \delta(\ell^+ \ell^- - \vec{\ell}_\perp^2) (-2\pi i) \delta \left[(\ell^+ + p_1^+) (\ell^- + p_2^-) - \vec{\ell}_\perp^2 - Q^2 \right] \\
&\times \left(\frac{-\vec{\ell}_\perp^2}{d-2} \right) \left[\frac{1}{(\ell^+ + p_1^+) \ell^- - \vec{\ell}_\perp^2} \right]^2 \\
&= \left(\frac{2\pi}{s} \right) \frac{1}{8\pi^2} \left(\frac{4\pi\mu^2}{Q^2} \right)^\epsilon \frac{z^\epsilon}{4} (1-z)^{1-2\epsilon} \frac{\Gamma(\epsilon)}{\Gamma(2-2\epsilon)} . \tag{30}
\end{aligned}$$

Compared to $I_{\text{sg(c)}}$, $I_{\text{cg(a)}}$ is suppressed by $\sim (1-z)^2 \sim \Lambda^2/Q^2$, so we can safely neglect this contribution. The suppression should occur since Fig. 3 (a) corresponds to the emission of collinear real gluon in the final state, which is forbidden by the end-point requirements. That is the reason for the suppression factor $(1-z)^2$. And Fig. 3 (b) gives the same result as Fig. 3 (a). It can also be easily found that

$$\mathcal{A}_{\text{cg(c)}} = -\mathcal{A}_{\text{cg(d)}} , \tag{31}$$

i.e., Figs. 3 (c) and (d) cancel each other. This is also true for their mirror images. Diagram Fig. 3 (e) vanishes because it is proportional to $\sim n^2(\bar{n}^2) = 0$ for $\bar{n}(n)$ -collinear gluon.

Note that the relevant contribution only comes from Fig. 2 (c). Using

$$(1-z)^{-1-2\epsilon} = \frac{1}{-2\epsilon}\delta(1-z) + \left[\frac{(1-z)^{-1-2\epsilon}}{1-z} \right]_+, \quad (32)$$

where ”+” denotes the usual plus distribution, we have in $\overline{\text{MS}}$ scheme

$$\begin{aligned} 2s \frac{d\sigma}{dQ^2} &= \left(\frac{2\pi}{s} \right) C^2(Q) \langle p\bar{p} | O_{DY} | p\bar{p} \rangle \left(\frac{g^2 C_F}{8\pi^2} \right) \left(\frac{4\pi\mu^2}{Q^2} \right)^\epsilon 2z^\epsilon (1-z)^{-1-2\epsilon} \frac{\Gamma^2(-\epsilon)}{\Gamma(1-\epsilon)\Gamma(-2\epsilon)} \\ &= \left(\frac{2\pi}{s} \right) C^2(Q) \langle p\bar{p} | O_{DY} | p\bar{p} \rangle \left(\frac{g^2 C_F}{8\pi^2} \right) \left[\frac{2}{\epsilon^2} \delta(1-z) + \frac{2}{\epsilon} \delta(1-z) \ln \frac{\mu^2}{Q^2} - \frac{4}{\epsilon} \left(\frac{1}{1-z} \right)_+ \right. \\ &\quad \left. + 8 \left(\frac{\ln(1-z)}{1-z} \right)_+ - 4 \left(\frac{1}{1-z} \right)_+ \ln \frac{\mu^2}{Q^2} + \delta(1-z) \left(\ln^2 \frac{\mu^2}{Q^2} - \frac{\pi^2}{2} \right) \right]. \end{aligned} \quad (33)$$

This is exactly the same as the full QCD result [3, 7], and [12].

IV. SOFT WILSON LINES

In this section we show how the above results can be described in terms of the soft Wilson line.

The differential cross section of DY process $p_1 + p_2 \rightarrow p_X + q$ is given by

$$\begin{aligned} 2s \frac{d\sigma}{dQ^2} &= \sum_X \int \frac{d^3 p_X}{(2\pi)^3} \frac{1}{2E_X} \int \frac{d^3 q}{(2\pi)^3} \frac{1}{E_q} \langle p\bar{p} | j^\mu(0) | X \rangle \langle X | j_\mu(0) | p\bar{p} \rangle (2\pi)^4 \delta^4(p_1 + p_2 - p_X - q) \\ &= \int \frac{d^3 q}{(2\pi)^3} \frac{1}{E_q} \int d^4 z e^{-iq \cdot z} \langle p\bar{p} | j^\mu(z) j_\mu(0) | p\bar{p} \rangle \\ &\equiv \int \frac{d^3 q}{(2\pi)^3} \frac{1}{E_q} 2\text{Im} W_{DY}, \end{aligned} \quad (34)$$

where

$$W_{DY} \equiv i \int d^4 z e^{-iq \cdot z} \langle p\bar{p} | T [j^\mu(z) j_\mu(0)] | p\bar{p} \rangle, \quad (35)$$

and T denotes the time ordering. The electromagnetic current j^μ is given by

$$\begin{aligned} j^\mu(z) &= \bar{\xi}_n W Y^\dagger C(\mathcal{P}_+) \gamma^\mu \bar{Y} \bar{W}^\dagger \chi_{\bar{n}}(z), \\ j_\mu(0) &= \bar{\chi}_{\bar{n}} \bar{W} \bar{Y}^\dagger C(\mathcal{P}_+) \gamma_\mu Y W^\dagger \xi_n(0) \end{aligned} \quad (36)$$

where $\mathcal{P}_+ = \mathcal{P} + \mathcal{P}^\dagger$ is the sum of label operators. Here the collinear and soft Wilson lines, W and Y , are explicitly factorized. Bars on the Wilson lines mean that the associated collinear direction is \bar{n} . In what follows, W 's are omitted since we are only interested in the soft Wilson lines. We adopt the convention of [18] for Y where the reference point of the Wilson

line is $-\infty$ uniquely. This notation is very convenient to check the universality of the cusp angles in the Wilson lines for various processes as can be seen later. The soft Wilson line Y is defined by

$$Y = \sum_{\text{perm}} \exp \left[-\frac{1}{n \cdot \mathcal{R} + i0^+} gn \cdot A_s \right], \quad (37)$$

where $\mathcal{R}^\mu = i\partial^\mu$ is the soft momentum operator. Its Fourier transformation is

$$Y(x) = P \exp \left[ig \int_{-\infty}^x ds n \cdot A_s(s) \right], \quad (38)$$

with P being the path ordering.

Using $j^\mu(z) = e^{i\hat{p}\cdot z} j^\mu(0) e^{-i\hat{p}\cdot z}$ where \hat{p} is the translation operator, the hadronic matrix element becomes ($C_+ \equiv C(\mathcal{P}_+)$)

$$\begin{aligned} W_{DY} &= i \int d^4z e^{-iq\cdot z} \langle p\bar{p} | T [e^{i(p_1+p_2)\cdot z} \bar{\xi}_n Y^\dagger C_+ \gamma^\mu \bar{Y} \chi_{\bar{n}}(0) e^{-i\hat{p}\cdot z} \cdot \bar{\chi}_{\bar{n}} \bar{Y}^\dagger C_+ \gamma_\mu Y \xi_n(0)] | p\bar{p} \rangle \\ &= \frac{i}{2} \int dz^+ dz^- (2\pi)^2 \delta^2(\vec{q}_\perp) \langle p\bar{p} | T \left[(\bar{\xi}_{n\alpha})_i C_+ (Y^\dagger \gamma_{\alpha\beta}^\mu \bar{Y})_{ij} (\chi_{\bar{n}\beta}(0))_j \right. \\ &\quad \left. \times e^{i(p_1^+ - q^+ - i\partial^+)z^-/2} e^{i(p_2^- - q^- - i\partial^-)z^+/2} (\bar{\chi}_{\bar{n}\rho})_l C_+ (\bar{Y}^\dagger (\gamma_\mu)_{\rho\lambda} Y)_{lm} (\xi_{n\lambda}(0))_m \right] | p\bar{p} \rangle \\ &= 2i(2\pi)^4 \delta^2(\vec{q}_\perp) C^2(Q) \frac{\delta^{im}}{N_c} \langle p | T [\bar{\xi}_{n\alpha} \xi_{n\lambda}] | p \rangle \gamma_{\alpha\beta}^\mu (\gamma_\mu)_{\rho\lambda} \frac{\delta^{lj}}{N_c} \langle \bar{p} | T [\bar{\chi}_{\bar{n}\rho} \chi_{\bar{n}\beta}] | \bar{p} \rangle \\ &\quad \times \langle 0 | T \left[(Y^\dagger \bar{Y})_{ij} \delta(p_1^+ - q^+ - i\partial^+) \delta(p_2^- - q^- - i\partial^-) (\bar{Y}^\dagger Y)_{lm} \right] | 0 \rangle, \end{aligned} \quad (39)$$

where $i, j, l, m, (\alpha, \beta, \rho, \lambda)$ are color(Dirac) indices and N_c is color number. The matrix elements are designed to be color singlet. We can write

$$W_{DY} = 2(2\pi)^4 \delta^2(\vec{q}_\perp) C^2(Q) \langle O_{DY} \rangle \cdot i S_{DY}, \quad (40)$$

where

$$\begin{aligned} \langle O_{DY} \rangle &= \frac{1}{N_c} \langle p | T [\bar{\xi}_{n\alpha} \xi_{n\lambda}] | p \rangle \gamma_{\alpha\beta}^\mu (\gamma_\mu)_{\rho\lambda} \langle \bar{p} | T [\bar{\chi}_{\bar{n}\rho} \chi_{\bar{n}\beta}] | \bar{p} \rangle, \\ S_{DY} &= \frac{1}{N_c} \text{Tr} \langle 0 | T [Y^\dagger \bar{Y} \delta(p_1^+ - q^+ - i\partial^+) \delta(p_2^- - q^- - i\partial^-) \bar{Y}^\dagger Y] | 0 \rangle. \end{aligned} \quad (41)$$

Here Tr means the trace over color. The appearance of double delta function in S_{DY} is a peculiar feature of DY process compared to others [11]. The nontrivial contribution of S_{DY} comes from one-loop diagram of Fig. 4. To make the soft-gluon loop, we first need the Feynman rule for the two soft gluon legs in Fig. 5. Expanding Y and \bar{Y} , we have

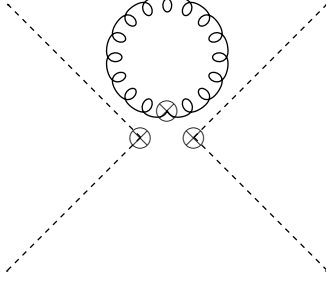


FIG. 4: Soft gluon one-loop contribution.

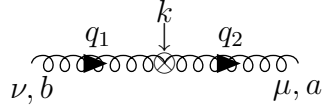


FIG. 5: S_{DY} at $\mathcal{O}(\alpha_s)$.

$$\begin{aligned}
& S_{DY}^{(2)} \\
&= \frac{g^2}{N_c} \text{Tr}(T^a T^b) \left\{ [\delta(k^+ + q_2^+ - q_1^+) \delta(k^- + q_2^- - q_1^-) + \delta(k^+) \delta(k^-)] \frac{\bar{n}^\mu}{\bar{n} \cdot q_2 - i0^+} \frac{n^\nu}{\bar{n} \cdot q_1 + i0^+} \right. \\
&\quad \left. + [\delta(k^+ - q_1^+) \delta(k^- - q_1^-) + \delta(k^+ - q_2^+) \delta(k^- - q_2^-)] \frac{n^\mu}{-n \cdot q_2 + i0^+} \frac{\bar{n}^\nu}{\bar{n} \cdot q_1 + i0^+} + (n \leftrightarrow \bar{n}) \right\}. \tag{42}
\end{aligned}$$

The superscript of $S_{DY}^{(2)}$ denotes the power of g . The decoupled soft gluon loop in Fig. 4 is

$$\begin{aligned}
S_{DY}^{\text{loop}} &= \frac{-ig^2}{N_c} \frac{\delta^{aa}}{2} \frac{n \cdot \bar{n}}{2} \int \frac{d^d q}{(2\pi)^d} \frac{1}{q^2 + i0^+} \left[2\delta(p_X^+) \delta(p_X^-) \frac{1}{q^+ - i0^+} \frac{1}{q^- + i0^+} \right. \\
&\quad \left. - \delta(p_X^+ - q^+) \delta(p_X^- - q^-) \left(\frac{1}{q^+ + i0^+} \frac{1}{q^- - i0^+} + \frac{1}{q^+ - i0^+} \frac{1}{q^- + i0^+} \right) + (q^\pm \rightarrow -q^\pm) \right]. \tag{43}
\end{aligned}$$

At this stage, recall that $d\sigma \sim 2\text{Im}W_{DY}$, and

$$\text{Im}W_{DY} = 2(2\pi)^4 \delta^2(\vec{q}_\perp) C^2(Q) \langle O_{DY} \rangle \text{Im}(iS_{DY}). \tag{44}$$

Terms proportional to $\delta(p_X^+) \delta(p_X^-)$ are zero in pure dimensional regularization. The remaining contributions give

$$\begin{aligned}
\text{Im}(iS_{DY}^{\text{loop}}) &= -2 \times g^2 C_F \frac{1}{2} \text{Im} \left[\int \frac{d\ell^+}{2\pi} \frac{d\ell^-}{2\pi} \frac{d^{d-2} \vec{\ell}_\perp}{(2\pi)^{d-2}} \frac{\delta(p_X^+ - \ell^+) \delta(p_X^- - \ell^-)}{\ell^+ \ell^- - \vec{\ell}_\perp^2 + i0^+} \frac{2}{\ell^+ \ell^-} \right] \\
&= -2 \times g^2 C_F \frac{1}{2(2\pi)^2} \int \frac{d^{d-2} \vec{\ell}_\perp}{(2\pi)^{d-2}} (-\pi) \delta(p_X^+ p_X^- - \vec{\ell}_\perp^2) \frac{2}{p_X^+ p_X^-} \\
&= \frac{g^2 C_F}{8\pi^2} \frac{(4\pi)^\epsilon}{\Gamma(1-\epsilon)} (p_X^+ p_X^-)^{-1-\epsilon}. \tag{45}
\end{aligned}$$

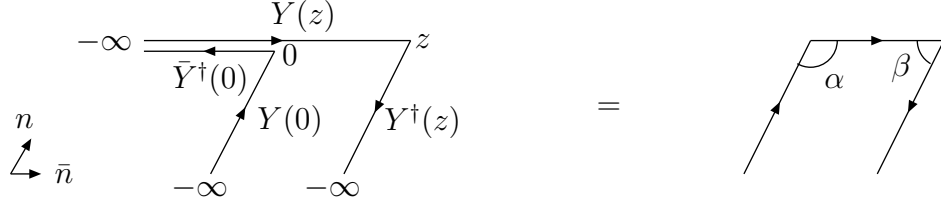


FIG. 6: Soft Wilson lines S_{DY} .

Here the sign-flipped terms yield the same result, and that is the reason of the overall factor

2. The differential cross section is

$$\begin{aligned}
2s \frac{d\sigma}{dQ^2} &= \int \frac{d^3 \vec{q}}{(2\pi)^3} \frac{1}{2E_q} 2\text{Im}W_{DY} \\
&= \int \frac{d^3 \vec{q}}{(2\pi)^3} \frac{1}{2E_q} 4(2\pi)^4 \delta^2(\vec{q}_\perp) C^2(Q) \langle O_{DY} \rangle \frac{g^2 C_F}{8\pi^2} \frac{(4\pi\mu^2)^\epsilon}{\Gamma(1-\epsilon)} (p_X^+ p_X^-)^{-1-\epsilon} . \quad (46)
\end{aligned}$$

The relevant phase space integral is

$$\begin{aligned}
&\int \frac{d^3 \vec{q}}{(2\pi)^3} \frac{1}{2E_q} (2\pi)^4 \delta^2(\vec{q}_\perp) (p_X^+ p_X^-)^{-1-\epsilon} \\
&= \int \frac{d^4 q}{(2\pi)^3} \delta(q^2 - Q^2) (2\pi)^4 \delta^2(\vec{q}_\perp) (p_X^+ p_X^-)^{-1-\epsilon} \\
&= (2\pi) \int d^4 p_X \delta[(p_1 + p_2 - p_X)^2 - Q^2] \delta^2(\vec{p}_X^\perp) (p_X^+ p_X^-)^{-1-\epsilon} \\
&= (2\pi) \frac{Q^\epsilon}{2} (p_2^-)^{-1-\epsilon} \int_0^{\frac{s-Q^2}{p_2^-}} dp_X^+ (p_X^+)^{-1-\epsilon} \left(\frac{s-Q^2}{p_2^-} - p_X^+ \right)^{-1-\epsilon} , \quad (47)
\end{aligned}$$

where we used the fact that $p_1^+ - p_X^+ = Q$ and $p_X^- = Q(1-x_2)/x_2 > 0$. Integral over p_X^\pm gives the beta function, and the final result is

$$2s \frac{d\sigma}{dQ^2} = \left(\frac{2\pi}{s} C^2(Q) \langle O_{DY} \rangle \right) \left(\frac{g^2 C_F}{8\pi^2} \right) \left(\frac{4\pi\mu^2}{Q^2} \right)^\epsilon 2z^\epsilon (1-z)^{-1-2\epsilon} \frac{\Gamma^2(-\epsilon)}{\Gamma(1-\epsilon)\Gamma(-2\epsilon)} . \quad (48)$$

This is exactly Eq. (33), since $\langle p\bar{p} | O_{DY} | p\bar{p} \rangle = \langle O_{DY} \rangle$.

The procedure implemented in this section can be explained geometrically by the universal cusp angle of the Wilson lines. Figure 6 shows S_{DY} . The resulting Wilson line (right one in Fig. 6) is just that of DIS [6, 11]. Thus the cusp angles are common in DY and DIS. Before cutting, the Wilson lines have two distinctive cusp angles, α and β . They are responsible for the cusp anomalous dimensions. What is different is the involved energy, $Q^2(1-z)^2 \sim \Lambda^2$ for DY and $Q^2(1-x) \sim QA$ for DIS. If we express S_{DY} in position coordinates, α and β have different $i\epsilon$ prescriptions for the corresponding eikonal lines. Taking a cut means dagger operation for β , resulting in two identical cusp angles [6].

The above picture is slightly different from [11]. Within the convention of [11] for the soft Wilson lines, there are two reference points, $\pm\infty$. In this convention, the hermiticity of the collinear spinor ξ_n is violated and a nontrivial factor $Y_\infty \equiv P \exp \left[ig \int_{-\infty}^{\infty} ds n \cdot A_s(s) \right]$ is involved [18]. The resulting Wilson lines for DIS and DY are quite different from those in this work or other literature, exhibiting two *identical* cusp angles (see Figs. 3(c) and 4(b) of [11]). Any kinds of cut operations are not needed in the soft Wilson lines afterward. The reason is that in the framework of [11], the soft Wilson lines do not have discontinuity at least at one loop level; the imaginary part of the hadronic tensor comes solely from the jet function from the construction. Also, the intermediate soft Wilson lines are chosen such that the relative extra factor Y_∞ between the two conventions does not appear, which results in the same physical observables. A more general discussion about the choice of convention can be found in [18].

V. DISCUSSIONS AND CONCLUSIONS

The finite part of soft gluon contributions to $d\sigma$ is (including tree level)

$$\begin{aligned}
F_{DY} &\equiv 2s \left(\frac{d\sigma}{dQ^2} \right)_{\text{finite}} / \left(\frac{2\pi}{s} C^2(Q) \langle O_{DY} \rangle \right) \\
&= \delta(1-z) + \left(\frac{\alpha_s C_F}{2\pi} \right) \left[8 \left(\frac{\ln(1-z)}{1-z} \right)_+ - 4 \left(\frac{1}{1-z} \right)_+ \ln \frac{\mu^2}{Q^2} \right. \\
&\quad \left. + \delta(1-z) \left(\ln^2 \frac{\mu^2}{Q^2} - \frac{\pi^2}{2} \right) \right].
\end{aligned} \tag{49}$$

The moment of F_{DY} is

$$\begin{aligned}
F_N &= \int_0^1 dz z^{N-1} F_{DY} \\
&= 1 + \left(\frac{\alpha_s C_F}{2\pi} \right) \left[8 \sum_{i=1}^{N-1} \frac{1}{i} \sum_{j=1}^i \frac{1}{j} + 4 \sum_{i=1}^{N-1} \frac{1}{i} \ln \frac{\mu^2}{Q^2} + \ln^2 \frac{\mu^2}{Q^2} - \frac{\pi^2}{2} \right] \\
&\rightarrow 1 + \left(\frac{\alpha_s C_F}{2\pi} \right) \left[4 \ln^2 \left(\frac{\mu}{Q} \frac{N}{N_0} \right) + \frac{\pi^2}{6} \right],
\end{aligned} \tag{50}$$

for large N . Here $N_0 = e^{-\gamma_E}$ where γ_E is the Euler number. In our picture, the large scale $\mu \sim Q$ determines lower and upper bounds for hard and soft physics, respectively [7].

The renormalization group equation (RGE) for F_N is

$$\left(\mu \frac{\partial}{\partial \mu} + \beta(g) \frac{\partial}{\partial g} \right) \ln F_N = \left(\frac{\alpha_s C_F}{\pi} \right) 2 \ln \left(\frac{\mu^2}{Q^2} \right), \tag{51}$$

where $Q' = QN_0/N$. The solution of RGE is simply

$$F_N(\mu) = F_N(Q') \exp \left[\int_{Q'^2}^{\mu^2} \frac{d\nu^2}{\nu^2} \left(\frac{\alpha_s(\nu^2)C_F}{\pi} \right) \ln \left(\frac{\nu^2}{Q'^2} \right) \right]. \quad (52)$$

Note that $\mu \geq Q' \sim \Lambda$. This is quite different from [12] where Q' is still large.

The counter term of the SCET current is [10, 12]

$$\text{c.t.} = \left(\frac{2\pi}{s} \langle O_{DY} \rangle \right) \left(\frac{g^2 C_F}{8\pi^2} \right) \left(-\frac{1}{\epsilon^2} - \frac{3}{2\epsilon} - \frac{1}{\epsilon} \ln \frac{\mu^2}{Q^2} \right) \delta(1-z). \quad (53)$$

Including Eq. (53), the divergent part of $d\sigma$ is

$$2s \left(\frac{d\sigma}{dQ^2} \right)_{\text{div}} + 2 \times \text{c.t.} = \left(\frac{2\pi}{s} \langle O_{DY} \rangle \right) \left(\frac{\alpha_s C_F}{-2\pi\epsilon_{IR}} \right) 2P_{q \rightarrow q}(z), \quad (54)$$

where

$$P_{q \rightarrow q}(z) \equiv C_F \left[\frac{3}{2} \delta(1-z) + 2 \left(\frac{1}{1-z} \right)_+ \right], \quad (55)$$

is the Altarelli-Parisi (AP) kernel. The infrared divergence is cancelled by the renormalized effective quark operator $O_n = \bar{\xi}_n \Gamma \xi_n$ where Γ is some gamma matrix. The corresponding renormalization constant is given by [10]

$$Z_n(x) = \delta(1-x) + \frac{\alpha_s}{2\pi\epsilon} P_{q \rightarrow q}(x). \quad (56)$$

The complete expression of $d\sigma$, including the SCET current counter terms, is

$$\begin{aligned} & \left[2s \left(\frac{d\sigma}{dQ^2} \right) + 2 \times \text{c.t.} \right] \\ &= \left(\frac{2\pi}{s} \right) C^2(\mu) \left[\delta(1-z) + \frac{\alpha_s}{2\pi} \left(\frac{1}{\epsilon} + \ln \frac{\mu^2}{Q^2} \right) 2P_{q \rightarrow q}(z) \right] \langle O_{DY} \rangle \cdot G(z) \\ &\equiv 2s \left(\frac{d\sigma}{dQ^2} \right)_{\text{NLO}}, \end{aligned} \quad (57)$$

where $G(z) - 1$ is the soft contribution,

$$G(z) = 1 + \left(\frac{4\pi\mu^2}{Q^2} \right)^\epsilon \left(\frac{\alpha_s C_F}{2\pi} \right) 2z^\epsilon (1-z)^{-1-2\epsilon} \frac{\Gamma^2(-\epsilon)}{\Gamma(1-\epsilon)\Gamma(-2\epsilon)}. \quad (58)$$

Here we specified $C = C(\mu)$ to show how the μ -dependence of Eq. (58) is cancelled. Plugging Eqs. (17) and (33) into (58), we have

$$\begin{aligned} & 2s \left(\frac{d\sigma}{dQ^2} \right)_{\text{NLO}} / \left(\frac{2\pi}{s} \right) \langle O_{DY} \rangle \\ &= \delta(1-z) + \frac{\alpha_s C_F}{2\pi} \left\{ 8 \left(\frac{\ln(1-z)}{1-z} \right)_+ + \delta(1-z) \left(-8 - \frac{\pi^2}{3} \right) \right. \\ &\quad \left. - \left[4 \left(\frac{1}{1-z} \right)_+ + 3\delta(1-z) \right] \ln \frac{\mu^2}{Q^2} + \frac{2P_{q \rightarrow q}(z)}{C_F} \ln \frac{\mu^2}{Q^2} \right\} \\ &= \delta(1-z) + \frac{\alpha_s C_F}{2\pi} \left\{ 8 \left(\frac{\ln(1-z)}{1-z} \right)_+ + \delta(1-z) \left(-8 - \frac{\pi^2}{3} \right) \right\}. \end{aligned} \quad (59)$$

Note that the μ -dependence of $C(\mu)$ combined with that of $G(z)$ is cancelled by the AP kernel of the quark operator [6].

In [5], factorization and resummation of Sudakov logs are analyzed in a general form. They also use the terminology "jet function" but the meaning is slightly different from that in SCET. In [5], the "jet" functions of DY scale as $Q/\mu N$ where N is the order of moments. These are the usual parton distribution functions, and correspond to $\langle O_{DY} \rangle$ in this work. The scaling behavior of the "jet" functions is the same as that of the "soft function", while the hard function scales as Q^2/μ^2 . On the other hand, the "jet" function of DIS scales as $Q/\mu N^{1/2}$ which exactly corresponds to the SCET jet function. The present work does not introduce the SCET jet functions in DY since no intermediate energy scale is assumed. The imaginary part of W_{DY} appears only in the soft Wilson lines.

Note that there is no scaling like $\sim N^{-1/2}$ in DY in full QCD. This is because no intermediate scale $\sim \sqrt{Q\Lambda}$ is assumed. The characteristic scaling of DY is N^{-1} which leads to a familiar correspondence $\Lambda/Q \sim 1-z \sim 1/N$ in QCD. In DIS where a large intermediate scale can exist, the Bjorken variable x scales at the end-point as $1-x \sim \Lambda/Q \sim 1/N \gg \Lambda^2/Q^2$, where the final state hadron has a large off-shellness, $p_X^2 = Q^2(1-x) \sim Q\Lambda \gg \Lambda^2$ [7, 10]. In [12], a similar relation holds, $1-z \sim 1/N$, but in this case $1-z \gg \Lambda/Q$ to make the intermediate scale $Q(1-z)$ large enough. Thus the moment scales as $\Lambda/Q \ll 1/N$ in [12], which might not be true for sufficiently large N . In this work, $1-z \sim \Lambda/Q \sim 1/N$ just like in QCD, as can be seen in Eq. (50). Consequently, $1-z$ behaves much better than that of [12] for large N , and our scaling behavior is consistent with the literatures.

In summary, DY process is analyzed in SCET near end-point. With the scaling of $Q(1-z) \sim \Lambda$, full QCD is directly matched onto SCET at $\mu = Q$. Previously well known results are successfully reproduced. In addition, it is shown that the soft Wilson line approach ensures that the factorization of soft gluon effects is automatic, and a single gluon loop diagram gives the same soft gluon corrections at $\mathcal{O}(\alpha_s)$. The structure of RGE is rather simple because there is no intermediate scale. It is also discussed how the scale dependence vanishes in the cross section.

[1] J.C. Collins, D.E. Soper, and G. Sterman, in *Perturbative Quantum Chromodynamics*, edited by A.H. Mueller (World Scientific, Singapore, 1989).

- [2] C.W. Bauer, S. Fleming and M.E. Luke, Phys. Rev. D **63**, 014006 (2001); C.W. Bauer, S. Fleming, D. Pirjol and I.W. Stewart, Phys. Rev. D **63**, 114020 (2001); C.W. Bauer and I.W. Stewart, Phys. Lett. B **516**, 134 (2001); C.W. Bauer, D. Pirjol and I.W. Stewart, Phys. Rev. D **65**, 054022 (2002).
- [3] G. Altarelli, R. K. Ellis and G. Martinelli, Nucl. Phys. B **157**, 461 (1979).
- [4] S. Catani and L. Trentadue, Nucl. Phys. B **327**, 323 (1989).
- [5] G. Sterman, Nucl. Phys. B **281**, 310 (1987); H. Contopanagos, E. Laenen and G. Sterman, Nucl. Phys. B **484**, 303 (1997) [arXiv:hep-ph/9604313].
- [6] G. P. Korchemsky and G. Marchesini, Nucl. Phys. B **406**, 225 (1993) [arXiv:hep-ph/9210281].
- [7] G. P. Korchemsky and G. Marchesini, Phys. Lett. B **313**, 433 (1993).
- [8] I. A. Korchemskaya and G. P. Korchemsky, Phys. Lett. B **287**, 169 (1992).
- [9] C. W. Bauer, S. Fleming, D. Pirjol, I. Z. Rothstein and I. W. Stewart, Phys. Rev. D **66**, 014017 (2002) [arXiv:hep-ph/0202088].
- [10] A. V. Manohar, Phys. Rev. D **68**, 114019 (2003) [arXiv:hep-ph/0309176].
- [11] J. Chay, C. Kim, Y. G. Kim and J. P. Lee, Phys. Rev. D **71**, 056001 (2005) [arXiv:hep-ph/0412110].
- [12] A. Idilbi and X. d. Ji, Phys. Rev. D **72**, 054016 (2005) [arXiv:hep-ph/0501006].
- [13] J. Chay and C. Kim, arXiv:hep-ph/0511066.
- [14] E. Lunghi, D. Pirjol and D. Wyler, Nucl. Phys. B **649**, 349 (2003) [arXiv:hep-ph/0210091].
- [15] T. Becher, R. J. Hill and M. Neubert, Phys. Rev. D **69**, 054017 (2004) [arXiv:hep-ph/0308122].
- [16] C. W. Bauer, D. Pirjol and I. W. Stewart, Phys. Rev. D **67**, 071502 (2003) [arXiv:hep-ph/0211069].
- [17] C. W. Bauer, A. V. Manohar and M. B. Wise, Phys. Rev. Lett. **91**, 122001 (2003) [arXiv:hep-ph/0212255]; C. W. Bauer, C. Lee, A. V. Manohar and M. B. Wise, Phys. Rev. D **70**, 034014 (2004) [arXiv:hep-ph/0309278].
- [18] C. M. Arnesen, J. Kundu and I. W. Stewart, Phys. Rev. D **72**, 114002 (2005) [arXiv:hep-ph/0508214].